Materials Science-Poland, 35(2), 2017, pp. 368-373
http://www.materialsscience.pwr.wroc.pl/
DOI: 10.1515/msp-2017-0043

DE GRUYTER OPEN

Kinetic properties and structural analysis of $LaCrO_3$ nanoparticles

MORTEZA ENHESSARI[1,*], ALI SALEHABADI[1], ASMA KHOOBI[2], RAZIE AMIRI[1]

[1]Department of Chemistry, Naragh Branch, Islamic Azad University, Naragh, Islamic Republic of Iran
[2]Department of Analytical Chemistry, Faculty of Chemistry, University of Kashan, Kashan, Islamic Republic of Iran

$LaCrO_3$ perovskite nanopowders were successfully prepared via a sol-gel method using stoichiometric proportion of materials containing lanthanum and chromium in stearic acid complexing agent. Structural analysis of $LaCrO_3$ indicated an octahedral framework in its XRD pattern bearing crystallite size in the range of 28 nm. The particle sizes were confirmed by morphological scanning of the sample. The optical properties of $LaCrO_3$ nanopowders clearly indicated an interesting optical activity of $LaCrO_3$ in the UV and visible ranges. The degradation activation energy (E_d) was calculated from the output of a moderate thermal programming profile at about 207.97 kJ·mol^{-1} using Kissinger equation. Capacity, impedance and AC resistance of the perovskites was obtained at 2.970 nF, 2.522 MΩ and 16.19 MΩ, respectively.

Keywords: *$LaCrO_3$; nanoperovskite; sol-gel; kinetic parameter*

1. Introduction

Knowledge on materials in the solid state chemistry is critical to understand the importance of many advanced materials [1]. The perovskite oxides containing rare earth ions have achieved a great interest due to their functional properties such as mixed conductivity caused by both ions and electron migration [2]. In the perovskite structure, the unit cell is not centrosymmetric, as the crystal grows in a permanent electric polarization. At a certain temperature, due to ions displacement, the perovskite can exhibit a cubic structure but of a lower symmetry, like a tetragonal unit cell at room temperature. High stability and selective sensitivity of ABO_3-type perovskite materials have an advantage that could be controlled by selecting suitable A and B atoms or by chemical doping [3]. $NiTiO_3$ [4, 5], $CoTiO_3$ [6, 7], $BaZrO_3$ [8], $LaMnO_3$ [9], $MnTiO_3$ [10], $PbTiO_3$ [11] are some examples of common perovskite oxides. The sol-gel process is one of the techniques among several reported techniques for preparation of perovskite materials [7, 12–15]. It is an appropriate technique for synthesis of dense nanomaterials with homogeneous texture and uniform morphology [16–19].

Several chromate compounds have been synthesized for various applications, for example, $MgCr_2O_4$ for humidity sensors [20], $NiCr_2O_4$ for optical devices [21], Ag_2CrO_4 and $Ag_2Cr_2O_7$ for catalytic properties [22], etc.

$LaCrO_3$ is regarded as a promising interconnector material for high temperature solid oxide fuel cells (SOFC) [23–25]. It has been reported that the polarization resistance using $LaCrO_3$ is high enough for efficient SOFC operation as no significant weight loss is observed. This implies that chromium strongly retains its six-fold coordination [26]. The kinetic parameters of perovskites used in SOFC are one of the most important factors influencing their performance. In acceptor-doped $LaMnO_3$, $LaCoO_3$, $LaFeO_3$, $LaCrO_3$, and donor-doped $BaTiO_3$, $SrTiO_3$ and $CaTiO_3$ perovskite materials there is always a linear correlation between the activation energy and the logarithm of the pre-exponential coefficient [27].

In current study, an attempt has been made to investigate a possible combination of the main element of lanthanide group – lanthanum – with

*E-mail: enhessari@iau-naragh.ac.ir

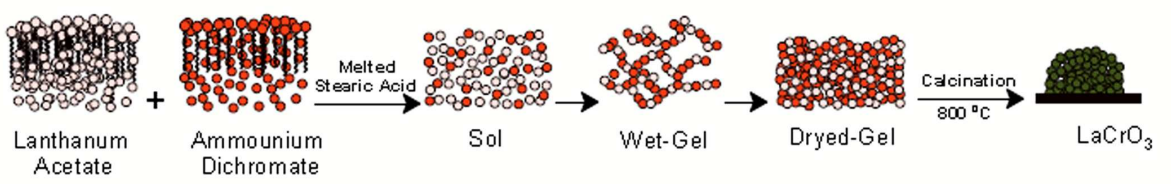

Fig. 1. Schematic representation of $LaCrO_3$ synthesis route.

a transition metal, chromium, to form $LaCrO_3$ perovskite oxides. Preparation method, i.e. sol-gel was the most prominent challenge in this study. Green-fine nanopowders were obtained after calcination at 800 °C and used for further analysis.

2. Experimental

2.1. Materials and method

A hydrated lanthanum acetate (a white crystalline powder, Mw = 316.04 g·mol^{-1}, 99.9 %, trace rare earth analysis $\leqslant$1500 ppm), ammonium dichromate (dark orange crystal, Mw = 252.06 g·mol^{-1}, 99.5 %), stearic acid (white paste, Mw = 284.48 g·mol^{-1}, 98.5 %, melting point = 67 °C to 73 °C) were all supplied by Sigma-Aldrich (US) and used as received.

Nanosized $LaCrO_3$ was synthesized using a modified sol-gel technique as shown in Fig. 1. Stochiometric amount of lanthanum acetate (0.04 mol) was dispersed in an appropriate amount of melted stearic acid, followed by immediate addition of 0.02 mol aqueous ammonium dichromate. After a careful stirring and complete evaporation of polar domain, a gel containing dispersed cations was obtained. A stepwise temperature programming consisting of continuous heating and holding was arranged in an electrothermal oven. The thermal treatment was started from 100 °C to 350 °C and finally the sample was calcined at 800 °C for 4 h. A mortar was used to grind the green product into the fine powder for further analysis.

2.2. Characterization

Infrared spectroscopic analysis of PHB, various PHB/MMT hybrids and MMT was carried out using PerkinElmer 2000 FT-IR apparatus. X-ray diffraction (XRD) patterns of the samples were obtained using the SIEMENS D5000 X-ray diffractometer and recorded in the range of 10° to 80°. The morphology of prepared $LaCrO_3$ nanopowders was characterized using a scanning electron microscopy (SEM, KYKY-EM3200) operating at an accelerating voltage of 26 kV. The UV-Vis diffuse reflectance spectroscopy (UV-Vis DRS) experiment was carried out using a UV-Vis Scinco 4100 spectrometer equipped with an integrating sphere reflectance accessory and $BaSO_4$ as a reference material.

The kinetic parameters were calculated by adsorption/desorption isotherms of N_2 at −196 °C using Chem-BET Pulsar TPR/TPD/BET (Toseye Hesgarsazan Asia Co., Iran). Typical degradation processes were investigated by temperature-programmed reduction (TPR) technique using a thermal conductivity detector (TCD) of a gas chromatograph (6890 plus, Toseye Hesgarsazan Asia Co., Iran). The sample was heated under gas flow rate of 10 K/min, 20 K/min and 30 K/min and held for 1 h at 1073 K to ensure complete metal reduction.

2.3. Kinetic study

Estimation of thermal properties, either thermal degradation or determination of the activation energy of the degradation process was desired for elucidating the thermal properties of $LaCrO_3$ nanoparticles. The activation energy of degradation (E_d) was calculated on the basis of TPR thermograms using Kissinger equations [28–30] without a precise knowledge of the reaction mechanism, equation 1:

$$-ln\frac{\beta}{T_p^2} = \frac{E_d}{RT_p} - ln\frac{AR}{E_d} \qquad (1)$$

where β is the heating rate (K/min), T_p is the maximum degradation temperature, E_d is the degradation activation energy, R is the gas constant and A is a pre-exponential factor. The plot of $-\ln\beta/T_p^2$ against $1/T_p$ gives a straight line. The E_d was obtained from the slope of the plot.

3. Results and discussion

3.1. Structural analysis

The FT-IR spectra of $LaCrO_3$ nanoparticles are presented in Fig. 2. The $LaCrO_3$ nanoparticles show a number of vibration frequencies below 1000 cm^{-1}. These absorption bands have been related to the metal-oxygen characteristic band, i.e. La–O and Cr–O vibration frequencies. In this frame, it was proven that the bands located at 618 cm^{-1} and 700 cm^{-1} originate from the stretching of Cr–O and bending of Cr–O–Cr bonds, while the contribution at 580 cm^{-1} results from La–O bonds. A characteristic band at around 408 cm^{-1} in the perovskite spectra indicate the metal-metal (La–Cr) vibration frequency.

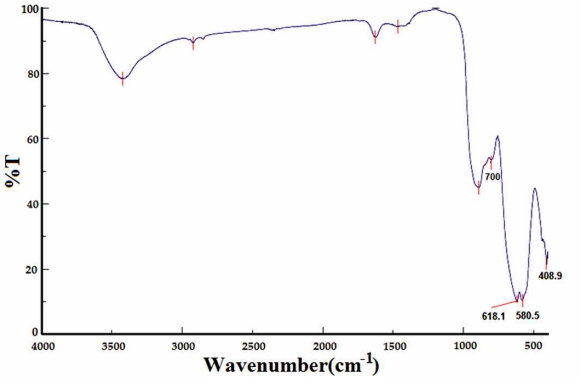

Fig. 2. FT-IR spectrum of $LaCrO_3$.

Fig. 3 shows the XRD pattern of $LaCrO_3$ nanopowders indexed within a perovskite structure (JCPDS Card No. 24-1016) having an orthorhombic crystal system with Pbnm space group (No. 62). Prominent in-plane lattice parameters of $LaCrO_3$ (1 1 0), (1 1 2) and (0 0 4) are 3.87 Å, 2.75 Å, and 1.94 Å located at 2θ equal to 17.93°, 32.59°, and 46.74°, respectively.

The crystallite size of the as-synthesized $LaCrO_3$, D, was calculated from the major diffraction peaks using Scherer [9] equation 2:

$$D = \frac{k\lambda}{\beta \cos\theta} \tag{2}$$

where K is a constant (ca. 0.9), λ is the X-ray wavelength (1.5418 Å), θ is the Bragg angle, β is the pure diffraction broadening of a peak at half-height, that is, broadening due to the crystallite dimensions. The estimated crystallite size of $LaCrO_3$ by the Scherrer equation is about 28 nm.

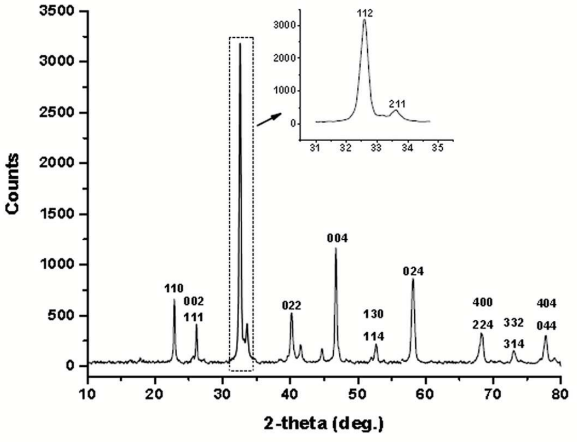

Fig. 3. XRD pattern of $LaCrO_3$ nanopowders.

3.2. Morphology analysis

In order to study the morphology and size of the synthesized nanopowders, the prepared nanocrystals were investigated by SEM, as shown in Fig. 4. SEM analysis indicates that $LaCrO_3$ nanoparticles with the diameter in the range of 35 nm to 55 nm are uniformly distributed. The particle sizes were measured using Digimizer.

3.3. UV-Vis diffuse reflectance spectra

To study the optical properties of $LaCrO_3$ nanopowders, the UV-Vis absorption spectrum of the nanoparticles was recorded (Fig. 5). The result clearly indicates interesting optical activity of $LaCrO_3$ in the UV and visible range. Two broad absorption edges at around 450 nm and 600 nm are associated with O 2p-Cr 3d(t_{2g}) and Cr

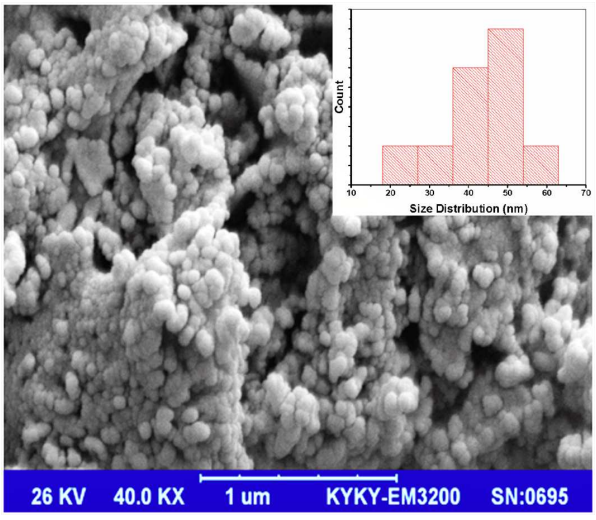

Fig. 4. SEM micrograph of $LaCrO_3$ nanoparticles.

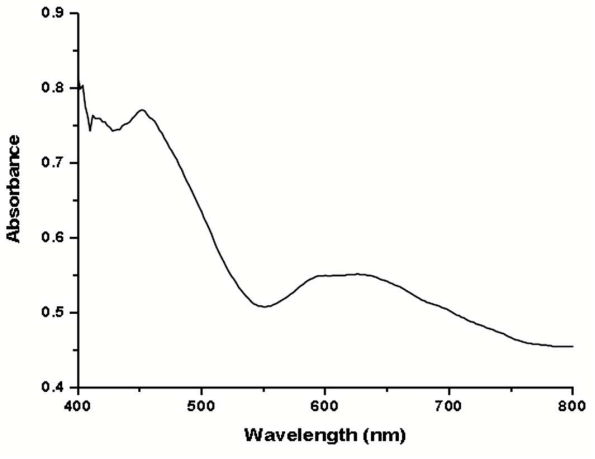

Fig. 5. UV-Vis diffuse reflectance spectrum of nanostructure $LaCrO_3$.

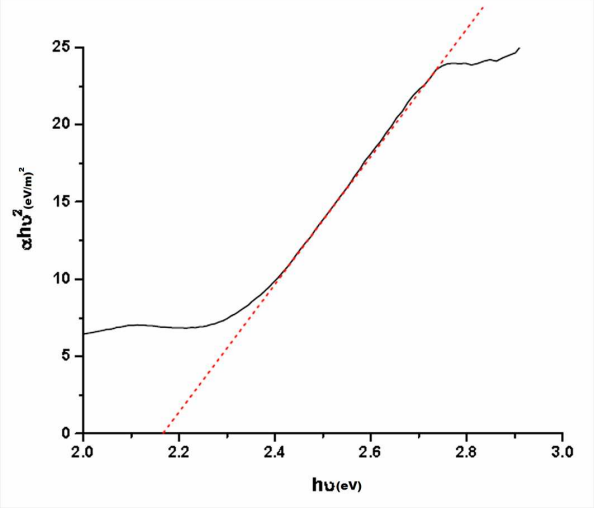

Fig. 6. Tauc plot for the calculation of direct band gap of nanostructure $LaCrO_3$.

$3d(t_{2g})$ to Cr $3d(e_g)$ transitions, respectively [31]. The absorbance peak at around 600 nm (due to the transition of Cr $3d(t_{2g})$ to Cr $3d(e_g)$) is important for photocatalytic activity. The photoinduced charge transfers of the nanosized $LaCrO_3$, required for photocatalytic reactions, can be ensured by several electronic transitions which further contribute to the efficient photocatalytic activity. The optical band gap (E_g) of $LaCrO_3$ was calculated using Tauc equation 3 [32]:

$$\alpha h\vartheta = A(h\vartheta - E_g)^n \tag{3}$$

where hν is the photon energy, α is the absorption coefficient, A is a constant related to the material, and n is either 2 for a direct transition or 1/2 for an indirect transition.

In this study, the photocatalyst was found to have direct band gap. Fig. 6 presents the Tauc plot, which shows the dependence of $(\alpha h\nu)^2$ vs. hν, where the intercept of the straight line on hν axis corresponds to the optical band gap. Therefore, the band gap of $LaCrO_3$ nanopowders is found at about 2.17 eV [33].

3.4. Kinetic parameters

Temperature-programmed reduction (TPR) is one of the quantitative techniques for investigating the reduction behavior of catalysts. In this study, TPR was used in the temperature range of 373 K to 1000 K to investigate the reduction behavior of the $LaCrO_3$ stability and kinetic parameters (Fig. 7). The sample does not show any reduction below ~520 K. Moreover, a single step reduction can be observed at around 773 K for the heating rate of 10 $K \cdot min^{-1}$, indicating highly pure nanopowders.

The Kissinger plot of $LaCrO_3$ nanoparticles is shown in Fig. 8. The value of E_d for the $LaCrO_3$ nanoparticles has been obtained from the slope of the linear curve at 207.97 kJ/mol. Moreover, the pre-exponential factor A has been estimated from the intercept of the curve according to equation 1.

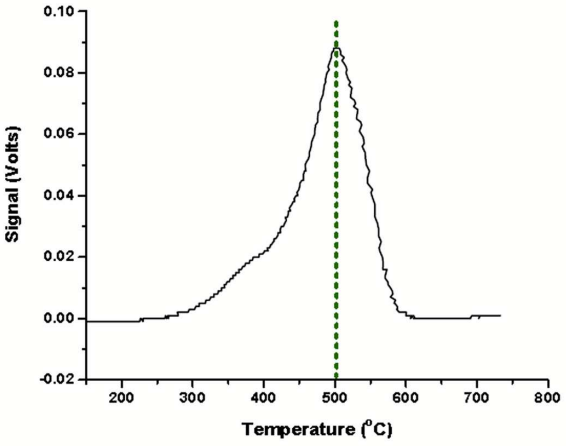

Fig. 7. TPR profile of $LaCrO_3$ nanoparticles at 10 K·min^{-1}.

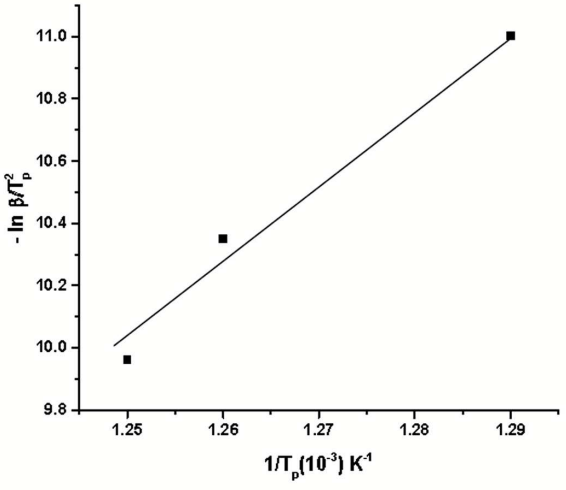

Fig. 8. Kissinger plot of $LaCrO_3$ nanoparticles.

3.5. Inductance, capacitance and resistance analysis (LCR test)

The electronic properties of $LaCrO_3$ were evaluated using LCR analyzer. The sample was subjected to an AC voltage source to determine the magnitude of impedance, inductance and resistance. The nanopowders were moulded into KBr-FT-IR disc shapes under appropriate pressure prior to analysis. The area and thickness of the disc was 1.327 cm^2 and 0.029 cm, respectively. Interestingly, the capacity, impedance and AC resistance of the $LaCrO_3$ nanopowders was obtained as 2.970 nF, 2.522 MΩ and 16.19 MΩ, respectively. The results clearly indicate that $LaCrO_3$ nanopowders can be used in high power electronic devices and diodes.

4. Conclusions

The $LaCrO_3$ nanopowders were synthesized via a sol-gel method. An appropriate combination of metal-oxygen and metal-metal cationic constitutions was observed at vibrational frequencies below 1000 cm^{-1}. The orthorhombic and pure perovskite structure indicated a successful formation of $LaCrO_3$. This was further confirmed by morphological observations. The estimated particle sizes of $LaCrO_3$ were ranging from 30 nm to 40 nm. The measured band gap of $LaCrO_3$ was calculated at about 2.17 eV. The photoinduced charge transfers of the nanosized $LaCrO_3$ contributed to the efficient photocatalytic activity. The E_d obtained from the Kissinger plot was calculated as 207.97 kJ/mol. The impedance measurements confirmed the semiconductor behavior of the perovskite oxide. The AC resistance of 16.19 MΩ obtained from LCR analysis may offer an effective route for designing sensors.

Acknowledgements

The authors thank the Iran Nanotechnology Initiative Council for supporting this project.

References

[1] ATKINS P., OVERTON T., ROURKE J., WELLER M., ARMSTRONG F., *Inorganic Chemistry*, New York, 2006.
[2] MORI M., ITAGAKI Y., SADAOKA Y., *Sensor. Actuat. B-Chem.,* 1 (2012), 44.
[3] POKHREL S., HUO L., ZHAO H., GAO S., *Sensor. Actuat. B-Chem.,* 1 (2007), 321.
[4] SADJADI M.S., MOZAFFARI M., ENHESSARI M., ZARE K., *Superlattice. Microst.,* 6 (2010), 685.
[5] SADJADI M.S., ZARE K., KHANAHMADZADEH S., ENHESSARI M., *Mater. Lett.,* 21 – 22 (2008), 3679.
[6] ENHESSARI M., PARVIZ A., OZAEE K., KARAMALI E., *J. Exp. Nanosci.,* 1 (2010), 61.
[7] ENHESSARI M., SALEHABADI A., NASROLLAHI Z., OZAEE K., *J. Semicond.,* 2 (2016), 0230021.
[8] ENHESSARI M., KHANAHMADZADEH S., OZAEE K., *J. Iran. Chem. Res.,* 1 (2010), 11.
[9] SHATERIAN M., ENHESSARI M., RABBANI D., ASGHARI M., *Appl. Surf. Sci.*, 2 (2014), 213.

[10] SHATERIAN M., BARATI M., OZAEE K., ENHESSARI M., *J. Ind. Eng. Chem.,* 1 (2013), 3646.
[11] ZARE K., SADJADI M.S., ENHESSARI M., KHANAHMADZADEH S., *J. Phys. Theor. Chem.* 1 (2009), 9.
[12] ENHESSARI M., SHATERIAN M., ESFAHANI M.J., Motaharian M.N., *Mat. Sci. Semicon. Proc.,* 6 (2013), 1517.
[13] SCHNELLER T., SCHOBER T., *Solid State Ionics,* 3 – 4 (2003), 131.
[14] SAHOO T., TRIPATHY S.K., NANDY S., PANDEY B., VERMA H.C., CHATTOPADHYAY K.K., ANAND S., *Mat. Sci. Eng. R,* 1 – 3 (2006), 277.
[15] MURAKOSHI K., *Sol. Energ. Mat. Sol. C.,* 1 – 2 (1998) 113.
[16] SALAVATI-NIASARI M., FARHADI-KHOUZANI M., DAVAR F., *J. Sol-Gel Sci. Technol.,* 3 (2009), 321.
[17] SALAVATI-NIASARI M., DAVAR F., FARHADI M., *J. Sol-Gel Sci. Technol.,* 1 (2009), 48.
[18] MAZLOUM-ARDAKANI M., SALAVATI-NIASARI M., KHAYAT-KASHANI M., GHOREISHI S.M., *Anal. Bioanal. Chem.,* 6 (2004), 1659.
[19] NOORI E., MIR N., SALAVATI-NIASARI M., GHOLAMI T., MASJEDI-ARANI M., *J. Sol-Gel Sci. Technol.,* 3 (2014), 544.
[20] DEBDULAL S., RUNA-MISTRY G., KUMAR K., KAMALENDU S., *Sensor. Actuat. B-Chem.,* 1 (2005), 323.
[21] ENHESSARI M., SALEHABADI A., KHANAHMADZADEH S., ARKAT K., NOURI J., *High. Temp. Mat. Proc.*, 1 (2016), 1.
[22] SOOFIVAND F., MOHANDES F., SALAVATI-NIASARI M., *Micro. Nano. Lett.*, 3 (2012) 283.
[23] YAKABE H., YASUDA I., *J. Electrochem. Soc.,* 1 (2003), A35.
[24] INOUE S., NONAKA H., SAITO T., YODA M., NAKAO T., TAKUWA Y., *ECS T.,* 1 (2015), 1589.
[25] ZHANG K.H.L., DU Y., PAPADOGIANNI A., BIERWAGEN O., SALLIS S., PIPER L.F.J., BOWDEN M.E., SHUTTHANANDAN V., SUSHKO P.V., CHAMBERS S.A., *Adv. Mater.,* 35 (2015), 5191.
[26] JIANG S.P., LIU L., ONG K.P., WU P., LI J., PU J., *J. Power Sources,* 176 (2008), 82.
[27] ISHIHARA T., *Oxide Ion Conductivity in Perovskite Oxide for SOFC Electrolyte,* in: ISHIHARA T. (Ed.), *Perovskite Oxide for Solid Oxide Fuel Cells,* Springer, New York, 2009, 65.
[28] SALEHABADI A., Abu Bakar M., *Mater. Sci. Forum,* 756 (2013), 119.
[29] SALEHABADI A., ABU BAKAR M., *Adv. Mater. Res.,* 623 (2013), 263.
[30] SALEHABADI A., BAKAR M.A., *Adv. Mater. Res.,* 844 (2014), 229.
[31] SILVA C.G., BOUIZI Y., FORNÉS V., GARCÍA H., *J. Am. Chem. Soc.,* 38 (2009), 13833.
[32] NASHIM A., PARIDA K., *J. Mater. Chem. A,* 43 (2014), 18405.
[33] NASHIM A., MARTHA S., PARIDA K.M., *RCS Adv.,* 28 (2014), 14633.

Received 2016-01-10
Accepted 2017-02-19